Cell

SKAR Links Pre-mRNA Splicing to mTOR/S6K1-Mediated Enhanced Translation Efficiency of Spliced mRNAs

Xiaoju Max Ma,[1] Sang-Oh Yoon,[1] Celeste J. Richardson,[1] Kristina Jülich,[1] and John Blenis[1,*]
[1]Department of Cell Biology, Harvard Medical School, 240 Longwood Avenue, Boston, MA 02115, USA
*Correspondence: jblenis@hms.harvard.edu
DOI 10.1016/j.cell.2008.02.031

SUMMARY

Different protein complexes form on newly spliced mRNA to ensure the accuracy and efficiency of eukaryotic gene expression. For example, the exon junction complex (EJC) plays an important role in mRNA surveillance. The EJC also influences the first, or pioneer round of protein synthesis through a mechanism that is poorly understood. We show that the nutrient-, stress-, and energy-sensing checkpoint kinase, mTOR, contributes to the observed enhanced translation efficiency of spliced over nonspliced mRNAs. We demonstrate that, when activated, S6K1 is recruited to the newly synthesized mRNA by SKAR, which is deposited at the EJC during splicing, and that SKAR and S6K1 increase the translation efficiency of spliced mRNA. Thus, SKAR-mediated recruitment of activated S6K1 to newly processed mRNPs serves as a conduit between mTOR checkpoint signaling and the pioneer round of translation when cells exist in conditions supportive of protein synthesis.

INTRODUCTION

In higher eukaryotes, most protein-coding genes are interrupted by introns. In the nucleus, splicing machinery removes introns from nascent pre-mRNA transcripts before the mRNAs are exported to the cytoplasm for translation. In addition to creating translatable mRNAs, splicing also facilitates later events in mRNA metabolism, including export, subcellular localization, mRNA surveillance, and protein synthesis (reviewed in Reed and Cheng, 2005; Le Hir et al., 2003; Lejeune and Maquat, 2005; Wilkinson, 2005).

The act of splicing "imprints" mRNA with a special set of proteins, which are multisubunit complexes including the TREX complex and the exon-junction complex (EJC) (reviewed in Tange et al., 2004; Reed and Cheng, 2005). The major nuclear cap-binding heterodimer CBP80/20 (major components of the cap binding complex or CBC) binds to the 5′ cap of pre-mRNA cotranscriptionally and is also required for efficient splicing (Izaurralde et al., 1994). Splicing recruits the TREX components, such as UAP56 and Aly/REF, to spliced mRNA near the CBP80/20-bound cap and facilitates mRNA export (Cheng et al., 2006). Splicing also recruits the EJC, which is formed ~20 nucleotides (nts) upstream of each exon-exon junction on spliced mRNA (Le Hir et al., 2000). Like CBP80/20, the EJC proteins are nucleocytoplasmic shuttling proteins that remain bound to mRNA after the mRNA-protein (mRNP) complex is exported to the cytoplasm (Kataoka et al., 2000; Dostie and Dreyfuss, 2002). Consistently, nuclear and cytoplasmic CBP80-bound mRNPs coimmunoprecipitate the EJC proteins (Ishigaki et al., 2001; Lejeune et al., 2002). The removal of EJCs from mRNA occurs after the first passage of ribosomes, a process known as the "pioneer" round of translation (Ishigaki et al., 2001; Wang et al., 2001; Dostie and Dreyfuss, 2002; Lejeune et al., 2002). During or after the pioneer round of translation, CBP80/20 is replaced by the major cytoplasmic cap-binding protein eIF4E (Ishigaki et al., 2001; Lejeune et al., 2002; Chiu et al., 2004).

The EJC functions to eliminate mRNAs with premature termination codons (PTCs), a process known as mRNA surveillance (reviewed in Lejeune and Maquat, 2005), and enhances protein synthesis of normal mRNAs (Wiegand et al., 2003; Nott et al., 2004; Gudikote et al., 2005). The stable core of the EJC contains four proteins: eukaryotic initiation factor 4AIII (eIF4AIII), Magoh, Y14, and MLN51 (also known as Barentsz), while other EJC proteins associate peripherally with the heterotetrameric core (reviewed in Tange et al., 2004). The peripheral EJC proteins identified so far include splicing coactivators (SRm160, RNPS1, and Pinin), mRNA surveillance factors (Upf3a, Upf3b, and Upf2), and some recently identified factors with unknown function (Acinus and SAP18) (reviewed in Tange et al., 2004; Chang et al., 2007). When a PTC occurs > 50-55 nts upstream of an exon-exon junction, the pioneer round of translation does not remove the EJCs downstream of the PTC, which ultimately triggers nonsense-mediated decay (NMD) of the mRNA (reviewed in Lejeune and Maquat, 2005).

Following the pioneer round of translation, mRNAs bound with eIF4E undergo steady-state translation. The rate-limiting step in the process of protein synthesis is translation initiation (reviewed in Gingras et al., 1999). Critical to this, eIF4E recruits eIF3 and the 40S ribosomal subunit to the 5′ end of mRNA. Several of the initiation steps are regulated by the mammalian target-of-rapamycin complex 1 (mTORC1). mTORC1 signaling, a positive regulator of protein synthesis which can be inhibited by rapamycin, is responsive to cellular energy status, nutrient availability, stress and the presence of growth factors. Under cellular conditions

supportive of protein synthesis, mTORC1 signaling to its major downstream effectors is initiated by its binding to eIF3 and the translation preinitiation complex where hypophosphorylated eIF4E binding proteins (4E-BPs) and the 40S ribosomal subunit protein S6 (rpS6) protein kinases (S6Ks) reside. Recruitment of mTORC1 into proximity of 4EBP1 leads to its phosphorylation and dissociation from eIF4E, resulting in the recruitment of the scaffold protein eIF4G, the RNA helicase eIF4A and poly(A)-associated poly(A)-binding protein PABP1 into the translation preinitiation complex (Gingras et al., 2001; reviewed in Hay and Sonenberg, 2004). mTORC1 binding to eIF3 also results in phosphorylation and dissociation of S6K1. Once activated, S6K1 phosphorylates rpS6 and eIF4B (reviewed in Fingar and Blenis, 2004). Phosphorylated eIF4B is recruited to eIF4A in the translation preinitiation complex (Holz et al., 2005). Finally, S6K1 also phosphorylates the tumor suppressor, PDCD4, an inhibitor of eIF4A. This phosphorylation event results in recruitment of the E3 ubiquitin ligase, βTRCP, leading to ubiquitination and degradation of PDCD4 (Dorrello et al., 2006). The S6K1 coordinated phosphorylation and recruitment of eIF4B to eIF4A and phosphorylation and degradation of PDCD4 is thought to greatly enhance eIF4A helicase activity, which facilitates 40S ribosomal subunit scanning to the initiation codon (Methot et al., 1996).

It has long been known that the presence of one or more introns in a gene, and therefore splicing, enhances gene expression (Callis et al., 1987; Palmiter et al., 1991; Braddock et al., 1994; Matsumoto et al., 1998; Lu and Cullen, 2003). EJC deposition is sufficient and necessary for a splicing-dependent increase in gene expression, potentially by enhancing association of spliced mRNAs with polysomes (Wiegand et al., 2003; Nott et al., 2004). Moreover, efficient splicing strongly promotes translation, which leads to an enhanced NMD response if a PTC is present in a gene (Gudikote et al., 2005). This suggests that efficient splicing may have evolved to enhance both steady-state translation and the pioneer round of translation through splicing-dependent formation of the EJC. Despite these recent advances in our understanding of the function of the EJC, the molecular mechanisms by which the EJC enhances protein synthesis remain poorly understood.

While much has been learned about the regulatory mechanisms of steady-state translation, it is unclear whether or how the pioneer round of translation of newly spliced mRNAs is regulated. This is due at least in part to the fact that the pioneer initiation complex is different from the steady-state initiation complex. Dynamic mRNP remodeling occurs during or after translation of CBP80-bound mRNAs so that the EJC proteins are undetectable in the eIF4E-bound mRNPs (Ishigaki et al., 2001; Lejeune et al., 2002; Chiu et al., 2004). However, the CBP80-bound mRNPs contain some components that also function during steady-state translation initiation, such as eIF4G, eIF4A, eIF2α, and eIF3 (Ishigaki et al., 2001; Lejeune et al., 2002, 2004; Chiu et al., 2004), suggesting that the assembly of the pioneer initiation complex could also be a rate-limiting step when translation machinery encounters newly spliced mRNAs.

Based on the above description of the important regulatory functions associated with the splicing-dependent assembly of the EJC and the role of the EJC in mRNA quality control and enhanced translational yield, we hypothesized that this process must be carefully monitored and regulated in the cell. Since protein synthesis is exquisitely sensitive to nutrient availability, energy status, stress responses and growth stimuli, we investigated the possible link between mTOR signaling, which is precisely regulated under these various conditions, and splicing-modulated protein synthesis.

Consistent with our hypothesis, we found that rapamycin inhibited the increase in translation efficiency gained by splicing. This finding suggested the possibility that mTOR and S6K1 might contribute to the assembly of an efficient pioneer initiation complex on CBP80-bound mRNA in response to environmental cues. Since the formation of the EJC is tightly linked to this process, we then asked if the EJC was somehow coupling mTOR signaling to this process. We show that an S6K1 specific interactor SKAR (S6K1 Aly/REF-like substrate), a cell growth regulator of unknown function (Richardson et al., 2004), is associated with CBP80-bound mRNP in a splicing-dependent manner. Mapping of the SKAR binding site on mRNA localizes SKAR to the EJC. Knockdown of SKAR or the core EJC component, eIF4AIII, results in a decrease of activated S6K1 associated with CBP80-bound mRNP and a reduction in the phosphorylation of the mRNP associated proteins. Finally, knockdown of S6K1, SKAR, and eIF4AIII leads to a similar decrease in the translation efficiency of spliced mRNAs. Our data show that the EJC serves an important function in linking mTOR signaling to the function of the pioneer initiation complex, that the S6K1 interactor, SKAR, is a component of the EJC, and that mTOR/S6K1 signaling contributes to the enhanced translation efficiency gained by splicing.

RESULTS

Linking mTOR Signaling to Protein Phosphorylation of CBP80-Bound mRNPs

Considering that an efficient translation initiation complex formed on newly spliced mRNAs is critical for the pioneer round of translation, we investigated whether the mTOR pathway modifies components of CBC-mRNPs by regulating their phosphorylation. We immunopurified CBC-mRNPs from serum-starved, insulin-stimulated, or rapamycin-pretreated HEK293E cells using anti-CBP80 antibody. The immunocomplexes were resolved by SDS-PAGE, and potential mTOR/S6K1 pathway targets in these complexes were identified by western blot using a motif antibody which recognizes a consensus sequence found in many of Akt or S6K1 substrates: phospho-Ser/Thr preceded by Lys/Arg at positions −5 and −3 (RXRXXpS/T). As shown in Figure 1A, a number of phosphoproteins associated with CBP80-bound mRNPs appeared with insulin stimulation, and most of these phosphorylation events were rapamycin sensitive. This suggests that the phosphorylation of these proteins is regulated by the mTOR pathway.

To support a role for mTOR/S6K1 signaling in pioneer translation initiation, we examined the presence of mTOR and S6K1 in CBP80-bound mRNPs. To this end, HEK293E cells were transiently transfected with HA-tagged CBP80, and mRNPs were immunoprecipitated using anti-HA antibody and, in parallel, anti-eIF4E antibody. Since the eIF3 complex acts as a scaffold for mTOR and S6K1 binding during translation initiation (Holz et al., 2005), proteins coimmunoprecipitated with the eIF3b

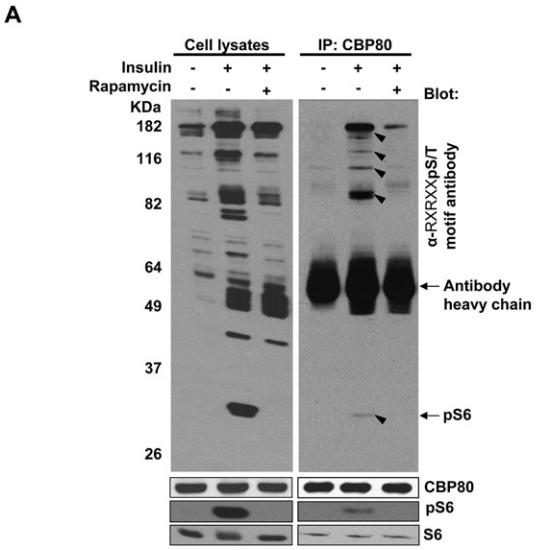

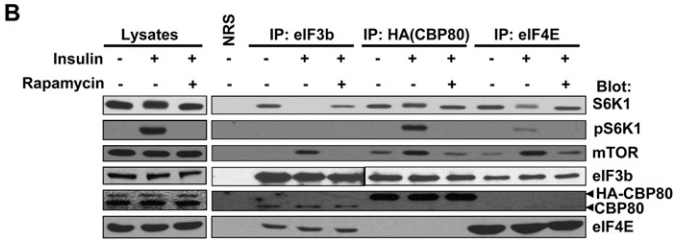

Figure 1. Rapamycin-Sensitive mTOR/S6K1 Signaling on CBP80-Bound mRNPs

(A) Phosphorylation of putative S6K1 substrates in CBP80-bound mRNPs. CBP80-bound mRNPs were immunoprecipitated (IP) using anti-CBP80 antibody from cells treated as indicated. The phosphorylation of putative S6K1 substrates was determined by immunoblotting with anti-RXRXXpS/T motif antibody. Immunoblotting with anti-phospho-S6 (Ser 240/244) antibody was performed to confirm the recognition of phospho-S6 by the motif antibody. Potential S6K1 substrates were indicated with arrowheads.

(B) Activated S6K1 and mTOR interact with CBP80-bound mRNPs. HEK293E cells were transfected with HA-tagged CBP80. Forty-eight hours posttransfection, the eIF3 complex, and mRNPs associated with HA-CBP80 or eIF4E were immunoprecipitated as described and their interaction with mTOR and S6K1 determined by immunoblotting. Normal rabbit serum (NRS) was used as a negative control in the experiments. These data are representative of greater than three experiments. Note that due to differences in the amount of eIF3 in the eIF3b IPs versus the HA-CBP80 and eIF4E IPs, thus resulting in differences in exposure times, the eIF3b immunoblots have been spliced together.

subunit served as controls. As shown in Figure 1B, mTOR was found to be enriched in both CBP80 and eIF4E immunocomplexes following insulin stimulation. Following phosphorylation and dissociation from the eIF3 complex, there was a reduction in the amount of activated S6K1 associated with eIF4E-bound mRNPs upon insulin stimulation. Surprisingly though, activated S6K1 remained bound to CBP80-bound mRNPs suggesting a potentially unique connection between activated S6K1 and the regulation of the pioneer round of translation.

SKAR Is Preferentially Associated with CBP80-Bound mRNPs

Since hyperphosphorylated S6K1 is found in CBP80-bound mRNPs, we hypothesized that S6K1 interacting proteins in the mRNP may serve to bring S6K1 near its translational targets after S6K1 is activated and dissociated from the eIF3 complex. S6K1 would then be able to phosphorylate these proximally associated proteins in the CBC-mRNP complex. Previous studies identified SKAR, an S6K1 interacting protein with unknown function (Richardson et al., 2004). Importantly, SKAR selectively interacts with activated S6K1 and not S6K2 (Richardson et al., 2004). Thus it is possible that SKAR may serve to recruit S6K1 to CBC-mRNPs.

We first wanted to determine whether SKAR interacts with CBC-bound mRNPs or eIF4E-bound mRNPs. Interestingly, SKAR was preferentially coprecipitated with HA-CBP80 but not eIF4E (Figure 2A). Upf3b, an EJC factor found exclusively in CBP80-bound mRNPs (Ishigaki et al., 2001), served as a positive control. We also confirmed SKAR interaction with endogenous CBP80-bound mRNPs. As shown, anti-SKAR antibody coimmunoprecipitated endogenous CBP80, but not eIF4E (Figure 2B). These data suggest that SKAR preferentially associates with CBP80 or CBP80-bound mRNPs.

SKAR Is Associated with Spliced mRNPs

To understand if SKAR facilitates S6K1 functioning during the pioneer round of translation, we set out to investigate the molecular nature of the interaction between SKAR and CBP80-bound mRNPs. SKAR is primarily localized to the nucleus (Richardson et al., 2004). SKAR also exhibits a punctate staining pattern that resembles that of nuclear speckles, from which splicing factors are recruited to sites of transcription and splicing. To test this possibility, we performed double immunofluorescent staining of SKAR and splicing factor SC35, a molecular marker for nuclear speckles. As shown in Figure 3A, SKAR significantly colocalizes with SC35, suggesting that a function of SKAR in the nucleus might be related to splicing and mRNP biogenesis.

To determine if SKAR is linked to splicing and mRNP biogenesis, we asked if SKAR associates with spliceosomes and/or spliced mRNPs. We employed a well-established method coupling in vitro spliceosome assembly and affinity purification (Zhou et al., 2002; Jurica et al., 2002). We introduced HA-SKAR into cells, from which whole cell splicing extract was prepared (Kataoka and Dreyfuss, 2004). Spliceosomes were assembled by incubating the extract with ^{32}P-labeled adenovirus major late (AdML) pre-mRNA (Figure 3B). The pre-mRNA substrate bears MS2-binding sequences at the 3′ end, which serve as a purification tag when pre-incubated with MS2-MBP fusion protein. Spliceosomes were then affinity-selected by binding to amylose resin and eluted with maltose-containing buffers. MS2-tagged intronless AdML mRNA served as a negative control (Figure 3B). The RNA contents of the eluted products were separated on a denaturing urea-PAGE. As visualized by phosphorimager analysis, spliced mRNAs were accumulated after incubation, indicating that spliceosomes as well as mRNPs

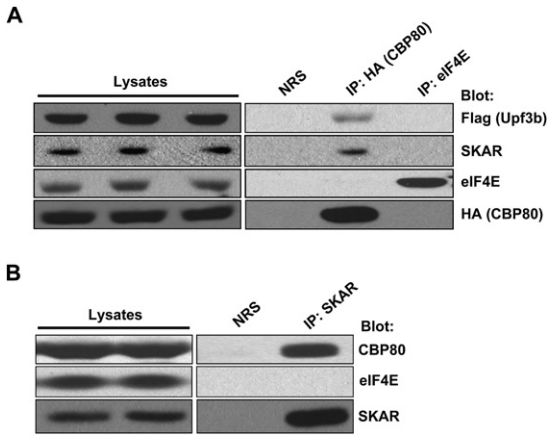

Figure 2. SKAR Is Preferentially Associated with CBP80-Bound mRNPs

(A) Immunoprecipitated CBP80-bound mRNPs contain SKAR. HEK293E cells were cotransfected with Flag-Upf3b and HA-CBP80. Twenty-four hours post-transfection, CBP80 and eIF4E mRNPs were immunoprecipitated. The association of SKAR and Flag-Upf3b with CBP80-bound mRNPs was determined by immunoblotting.

(B) SKAR coimmunoprecipitates endogenous CBP80. SKAR was immunoprecipitated and assayed for interaction with endogenous CBP80.

generated through splicing were affinity purified (Figure 3C, left panel). The protein contents of the eluted products were subjected to SDS-PAGE and western blotting. As expected, splicing factor SC35 was detected in purified spliceosomes but much less so in the control purification (Figure 3C, right panel), indicating that the spliceosomes were highly purified. We then examined whether SKAR was enriched in the purified spliceosomes and spliced mRNPs. As shown, SKAR also preferentially copurified with eluted spliceosomes and spliced mRNPs, and not with the intronless RNA control, suggesting that SKAR is associated with spliceosomes and/or spliced mRNPs, and that SKAR exhibits little nonspecific RNA binding activity despite the fact that it contains a highly conserved RNA recognition motif (RRM) (Richardson et al., 2004). To avoid potential complications resulting from high overexpression, HA-SKAR was expressed at levels below that of endogenous SKAR (Figure 3D).

Having detected SKAR in spliceosomes and/or spliced mRNPs, we wanted to further examine its binding to unspliced pre-mRNAs versus spliced mRNAs. For this purpose, endogenous SKAR was immunoprecipitated following in vitro splicing reactions and the RNA content of the precipitant was resolved by denaturing urea-PAGE to analyze the RNA species associated with SKAR. Remarkably, only spliced mRNAs coimmunoprecipitated with SKAR (Figure 3E), suggesting that SKAR preferentially associates with spliced mRNAs but not unspliced pre-mRNAs or intronless control mRNAs. Since Aly/REF is recruited to mRNA in a splicing-dependent manner (Cheng et al., 2006), its association with spliced mRNAs served as a positive control in this experiment. To test if the interaction between SKAR and the spliced mRNA is substrate-independent, Fushi tarazu (Ftz) pre-mRNA was used as an alternative substrate in the RNA coimmunoprecipitation analysis described above. Spliced Ftz mRNA was selectively coprecipitated by SKAR antibodies (Figure 3F). To examine whether SKAR recruitment to spliced mRNA is regulated by the mTOR pathway, splicing extracts were prepared from serum-starved, insulin-stimulated, or rapamycin-pretreated and insulin-stimulated HEK293E cells. However, no obvious difference on either splicing activity or mRNA binding efficiency of SKAR was observed (data not shown). These data, together with the finding that SKAR associates with CBP80-bound mRNP in the cell, indicate that SKAR is recruited to newly generated mRNPs in a splicing-dependent, substrate-independent manner.

SKAR Is Associated with the EJC

To gain further evidence for a possible role of SKAR in the pioneer round of translation, we next aimed to determine if SKAR is recruited to the EJC. Since the EJC binds tightly to a short sequence ~20 nts upstream of the exon-exon junction of spliced mRNAs, RNase digestion applied after the in vitro splicing reaction yields a short RNA oligonucleotide protected by the EJC (Le Hir et al., 2000). This EJC-bound RNA oligonucleotide was then subjected to coimmunoprecipitation analysis described in Figure 3E. To increase the sensitivity and specificity of this assay, we introduced a single ^{32}P-labeled nucleotide located 20 nt upstream of the 5′ splice site to AdML pre-mRNA substrate as previously described (Le Hir et al., 2000; Ma et al., 2003). Intronless AdML mRNA labeled at the equivalent position served as control. To ensure that the EJC-protected fragment was generated properly as a result of splicing, in vitro splicing reactions at different time points were treated with RNase A. As shown Figure 4A, the amounts of EJC-protected fragments (right panel) were proportional to spliced AdML mRNAs accumulated in the reactions (left panel), whereas the intronless control mRNAs did not yield any protected fragment following incubation under the same splicing conditions (Le Hir et al., 2000). This result confirmed that the RNA fragments specifically protected and bound by the EJC were successfully generated following splicing and RNase digestion. As shown in Figure 4B, the EJC-bound RNA fragment was coimmunoprecipitated by anti-SKAR antibody. As a negative control, antibodies against Aly/REF, a component of the TREX complex that binds near the 5′ end of spliced mRNA (Cheng et al., 2006), failed to coprecipitate the EJC-protected fragment. Antibodies against eIF4AIII, a core component of the EJC, were used as a positive control. We also tested whether SKAR interacts with EJC components in a similar RNase-resistant manner. As shown in Figure 4C, eIF4AIII was coimmunoprecipitated with SKAR, and the interaction was not disrupted by RNase digestion. Taken together, these results suggest that SKAR is associated with the EJC.

SKAR Shuttles between the Nucleus and Cytoplasm

To further characterize SKAR, we also wanted to determine if SKAR shuttles between the nucleus and cytoplasm. We employed a heterokaryon shuttling assay to test this possibility. Briefly, plasmids expressing HA-SKAR and GFP-tagged hnRNP C1, a non-shuttling factor serving as a negative control, were transiently cotransfected into human U2OS cells, which were then fused to non-transfected mouse NIH 3T3 cells to generate heterokaryons. Four hours after cell fusion, cells were stained with anti-HA antibodies to monitor the presence of HA-SKAR

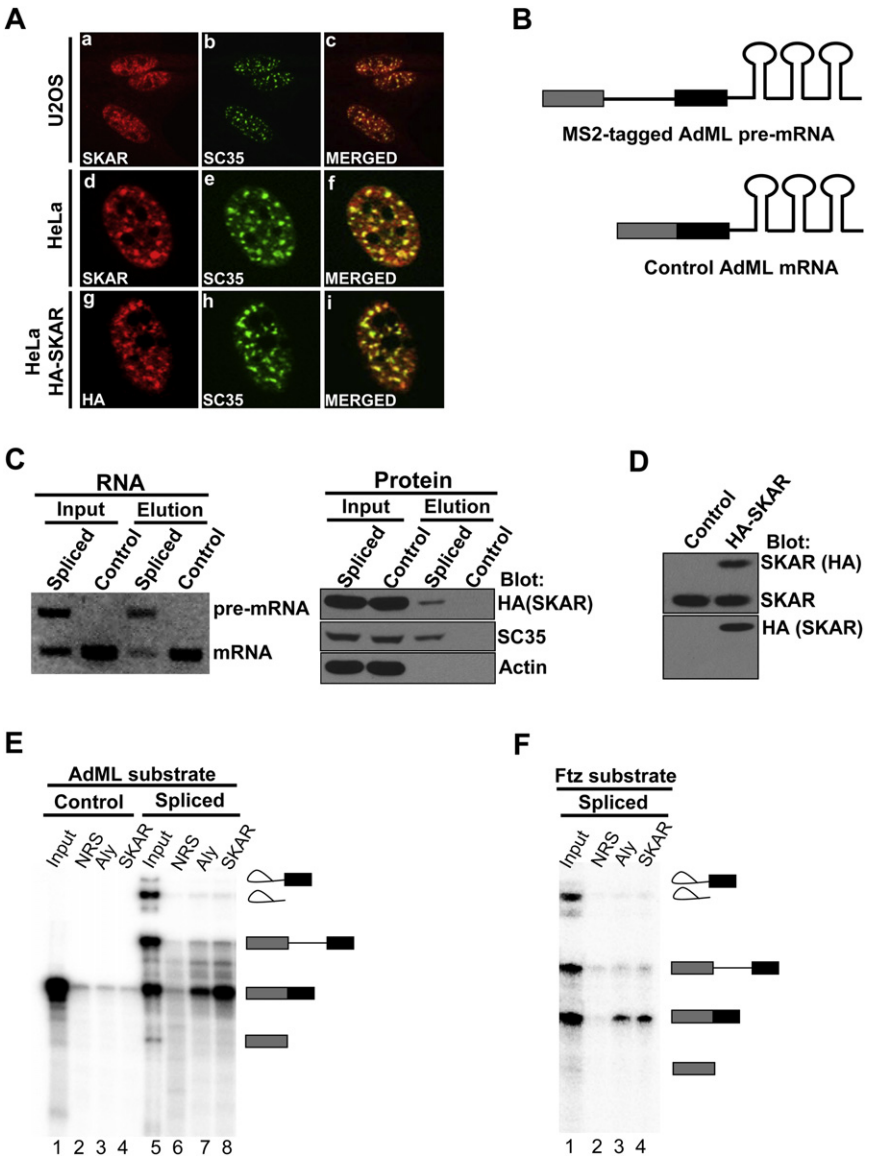

Figure 3. SKAR Is Preferentially Associated with Spliced mRNPs

(A) SKAR is concentrated in nuclear speckles. U2OS or HeLa cells were fixed and costained for SKAR (panels a and d), or HA-SKAR (g), and for SC35 to localize nuclear speckles (b, e, and h). A merge of the two images is shown with yellow indicating areas of colocalization (c, f, and i).

(B) Schematic of AdML pre-mRNA and intronless RNA control. MS2 is a bacteriophage protein, which recognizes the MS2 tag shown at the 3′ end of RNAs.

(C) SKAR copurifies with spliceosomes and/or spliced mRNPs. Left panel: Total RNAs from the initial splicing reaction (input), or eluted fractions from the amylose affinity resin (elution) were separated by 8% denaturing PAGE and visualized by phosphorimager analysis. Uniformly ^{32}P-labeled AdML pre-mRNA and spliced mRNA (spliced), and intronless mRNA (control) are indicated. Right panel: Immunoblotting of the initial splicing reaction (input), or eluted fractions (elution) using the indicated antibodies. These data are representative of greater than three experiments.

(D) The ratio between HA-SKAR and endogenous SKAR was shown by immunoblotting with anti-SKAR antibodies.

(E) SKAR is preferentially associated with spliced mRNA. Uniformly ^{32}P-labeled AdML pre-mRNA (lane 5) and intronless mRNA (lane 1) were both incubated for 90 min under splicing conditions, followed by immunoprecipitation with indicated antibodies. One-tenth of total reaction was loaded as input. RNAs were separated by 15% denaturing PAGE. Structures of splicing substrates, intermediates and products are diagrammed. These data are representative of greater than five experiments.

(F) Splicing reaction and immunoprecipitation were carried out as described in (E) except that uniformly ^{32}P-labeled Ftz pre-mRNA was used as splicing substrate.

in mouse nuclei. Human and mouse nuclei can easily be distinguished using DAPI staining, which appears speckled only in mouse nuclei (Figure 4D, right panel). As shown, HA-SKAR was detectable in the nuclei of mouse cells that have fused with human cells and not in mouse cells that have not undergone fusion (left panel). This data suggest that SKAR is a nucleocytoplasmic shuttling protein.

Effect of S6K1, SKAR, and eIF4AIII Knockdown on Putative S6K1 Targets in CBP80-Bound mRNPs

We wanted to test the hypothesis that the association of activated S6K1 with the pioneer initiation complex was needed for subsequent phosphorylation of CBP80-associated, mRNA binding proteins, and that SKAR may serve as a scaffold protein for recruitment of activated S6K1 to the newly spliced mRNA. To do this, we performed the phosphoprotein profiling analysis using the anti-RXRXXpS/T motif antibody as described in Figure 1A. To avoid contamination from antibodies used for immunoprecipitation, we introduced pNTAP vector expressing CBP80 with streptavidin binding peptide (SBP) and calmodulin binding peptide epitope tags into HEK293E cells and purified the associated mRNPs. As shown in Figure 5A (right panel), CBP80-bound mRNPs from S6K1 knockdown cells revealed reduced insulin-stimulated protein phosphorylation at RXRXXpS/T sites compared to the control knockdown cells, suggesting that many of these rapamycin-sensitive phosphoproteins, revealed by this phospho-specific motif antibody, were indeed targets of S6K1. Importantly, RNAi-mediated knockdown of SKAR also prevented the insulin-stimulated increase of the same phosphoproteins in CBP80-bound mRNPs (similar results were obtained with anti-HA-CBP80 immunoprecipitations, data not shown). Moreover, knockdown of S6K2, a homolog of S6K1, which does not interact with SKAR (Richardson et al., 2004), did not affect S6K1-dependent phosphorylations (Figures S2A

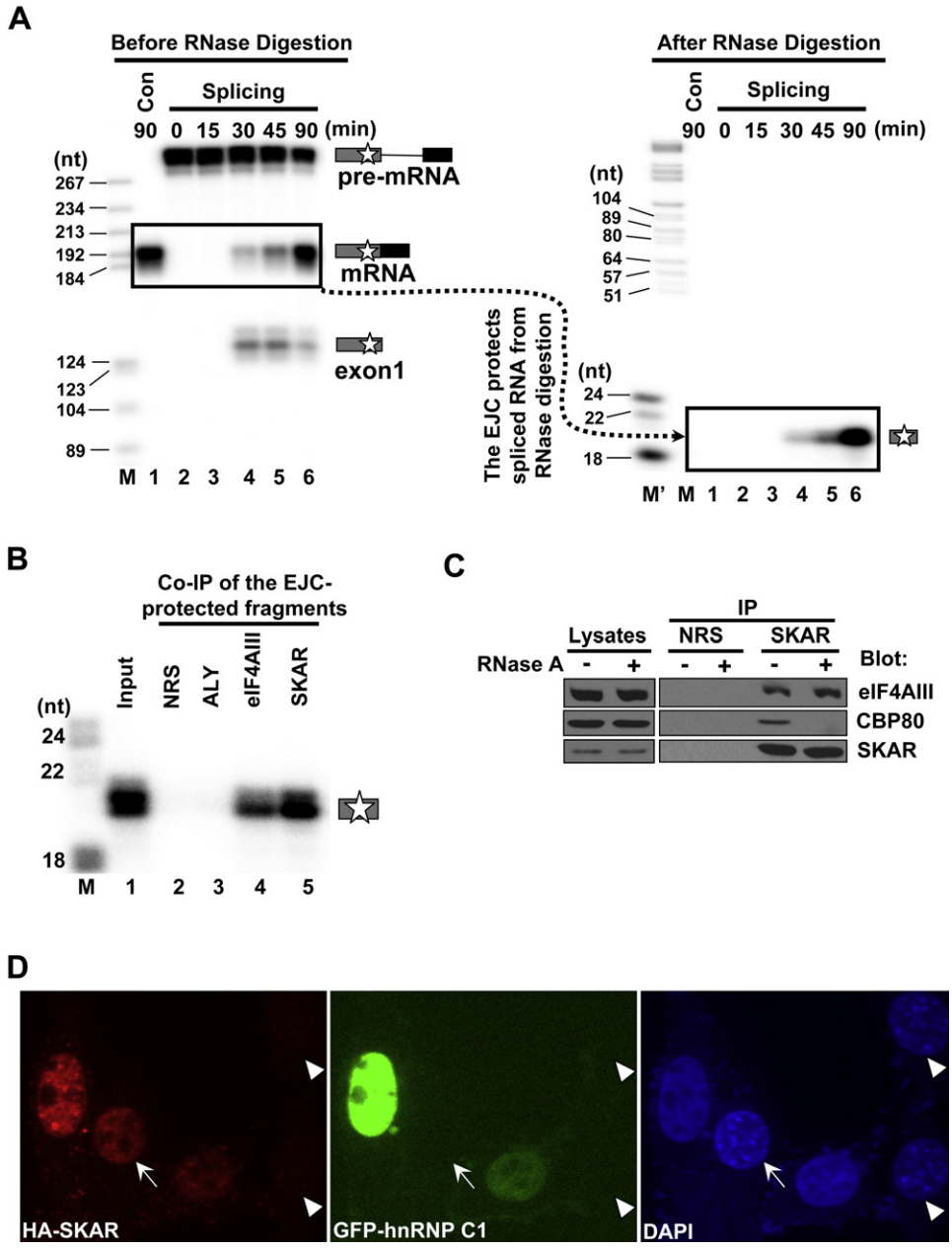

Figure 4. SKAR Is Deposited on the EJC and Shuttles to the Cytoplasm

(A) Generating the EJC-protected fragments. Splicing time courses for AdML pre-mRNA containing a site-specific ^{32}P label at 20 nt upstream of the 5′ splice site (left panel; lanes 2-6). "☆" represents the site-specific ^{32}P-label. "Con." stands for control AdML mRNA was labeled at the equivalent position and incubated under the same conditions for 90 min (left panel; lane 1). Complete RNase A digestion at each time point yielded the EJC-protected fragment of ~19 nt in length (right panel; lanes 4–6). RNA fragments were analyzed by a 20% denaturing PAGE.

(B) SKAR is associated with the EJC. The EJC-protected fragment was immunoprecipitated with the indicated antibodies. One-tenth of the input was loaded. The RNA fragment with the site-specific ^{32}P-label is illustrated. These data are representative of greater than three experiments.

(C) SKAR interacts with other components of the EJC in an RNase-resistant manner. SKAR was immunoprecipitated from cell lysates, and its interaction with eIF4AIII was determined by immunoblotting. RNase A treatment was carried out at 20°C for 20 min before adding antibody. CBP80 was used as the negative control under conditions where RNase digestion was applied.

(D) SKAR is a nucleocytoplasmic shuttling protein. Heterokaryons were produced as described in Experimental Procedures. Cells were stained with DAPI (right) and with anti-HA antibodies (left), while GFP-hnRNP C1 was directly visualized (middle). Arrowheads indicate mouse nuclei. A heterokaryon is shown by the arrow on the left.

and S2B). We also examined the association of activated S6K1 with CBP80-bound mRNPs in these cells. Following insulin stimulation, the level of total and activated S6K1 in CBP80-bound mRNPs was reduced in SKAR knockdown cells (Figure 5B), which is consistent with the reduced level of phosphorylation events in the mRNP. Knockdown of SKAR did not affect the small amount of activated S6K1 associated with eIF4E-bound mRNPs suggesting the possibility that S6K1 may also be recruited to the translation apparatus in a SKAR-independent mechanism, albeit at significantly lower levels (Figure 5B). We also determined whether disrupting formation of the EJC has a similar effect. The proper assembly of the EJC can be abolished by eliminating one of its core components eIF4AIII (Shibuya et al., 2004). As expected, phosphorylation of proteins in CBP80-bound mRNPs prepared from eIF4AIII knockdown cells was also greatly reduced (Figure 5C). Taken together, these results suggest that an intact EJC and SKAR contribute significantly to S6K1 phosphorylation of CBC-mRNPs.

S6K1, SKAR, and eIF4AIII Modulate Splicing-Dependent Increase in Translational Efficiency

Since the EJC enhances translational yield of spliced mRNA (Wiegand et al., 2003; Nott et al., 2004; Gudikote et al., 2005), we examined whether mTOR signaling contributes to the splicing-dependent increase in translational yield. HEK293E cells were transiently transfected with two plasmids: (1) one of two TPI/*Renilla* luciferase reporter constructs that encode either intronless or intron-containing *Renilla* mRNA; and (2) the firefly luciferase control plasmid (Figure 6A). The levels of firefly luciferase activity were used to control for variations in the efficiency of cell transfection. *Renilla* luciferase activities were normalized to corresponding firefly controls, and the ratio between intron-containing and intronless *renilla* luciferase activities served as an index for the enhanced translational yield gained by having an intron (see Experimental Procedures). Using this assay, we measured the effect of rapamycin on splicing-dependent increase in protein synthesis. As shown in Figure 6B (upper panel), rapamycin led to a significant decrease in intron-containing over intronless translation rates suggesting that a splicing-dependent increase in translation is modulated by mTOR signaling (similar results were obtained in mouse embryonic fibroblasts, data not shown). Semiquantitative RT-PCR analysis on intron-containing *renilla* and Firefly mRNAs revealed no obvious difference between the treatment groups (right panel) and similar results were observed for intronless *renilla* mRNAs (data not shown), suggesting that changes in luciferase activity were due mainly to changes in translational yield. To determine if S6K1, SKAR, and eIF4AIII can modulate a splicing-dependent increase in translational efficiency, we performed the luciferase reporter assay as described above using cell lines with gene-specific knockdowns. As shown in Figure 6C, knockdown of S6K1, SKAR, and eIF4AIII all led to a significant decrease in translational efficiency of the spliced-message without evidently affecting mRNA levels in these cells. Expression of an RNAi-immune form of SKAR partially rescued the decrease in translational efficiency due to knockdown of endogenous SKAR (Figure S3). Moreover, knockdown of S6K2 did not affect the translational efficiency of the spliced-message (Figure S2C). Therefore, S6K1, the EJC, and SKAR positively modulate the translational yield of intron-containing genes.

DISCUSSION

Under conditions of nutrient and energy sufficiency and the presence of growth factors that activate the mTOR pathway, the translation initiation complex should be more efficient in the translation of newly synthesized mRNAs. The enhanced efficiency of translating new mRNAs gained by mTOR activation is particularly important when a cell depends on production of specific effector proteins as a result of transcriptional activity in response to a variety of stimuli. S6K1, through its association with CBC-mRNPs may serve to ensure the efficiency and accuracy of gene expression when the cell exists in conditions supportive of protein synthesis.

The results reported in this study provide new information on several levels. We provide data detailing the molecular mechanism underlying splicing-dependent recruitment of SKAR, an activated S6K1-specific interacting protein, to CBP80-bound mRNPs. We have identified one binding site on the CBC-mRNP to be at the EJC. Through SKAR the EJC serves to facilitate the association of S6K1 with CBP80-bound mRNPs and to mediate subsequent phosphorylation events, potentially contributing to efficient translation initiation and/or elongation. Knockdown of SKAR or the EJC core component eIF4AIII leads to dissociation of active S6K1 from the CBP80-bound mRNP, loss of growth factor-stimulated, S6K1-mediated phosphorylations and a reduction of the translational yield gained by splicing. Together, our data give insight into the molecular mechanism underlying a splicing-dependent increase in translation efficiency and provide a new paradigm for understanding protein synthesis modulated by mTOR signaling.

How the EJC contributes to translation on newly synthesized mRNAs is unclear. Our results suggest the following model for how mTOR/S6K1 signaling contributes to enhanced translation efficiency of spliced mRNPs. Following an activation signal (e.g., insulin stimulation), mTOR/raptor is recruited to the eIF3 complex leading to phosphorylation of the bound and inactive S6K1 at its hydrophobic motif, resulting in its dissociation. PDK1 then binds S6K1 and phosphorylates its activation loop site resulting in an activated kinase (Holz et al., 2005). The EJC is required for splicing-dependent increase in protein synthesis (Wiegand et al., 2003; Nott et al., 2004; Gudikote et al., 2005). SKAR, which is located within the EJC, can then serve to recruit activated S6K1 to the CBC-mRNP. In this way, activated S6K1 is placed in proximity of additional translational targets, a process that may contribute to the efficient assembly and activation of the pioneer translation complex through S6K1-mediated phosphorylation events. Which proteins are phosphorylated and how they function remains to be determined. By database analysis, several candidate targets with potential S6K1 phosphorylation sites are revealed including some previously identified (reviewed in Hay and Sonenberg, 2004) that can be found in various complexes along the CBC-mRNP. Interestingly, Y14, a core component of the EJC was previously described to interact with Aly/REF (Kataoka et al., 2001) and we have found that SKAR interacts with Aly/REF in a two-hybrid screen using

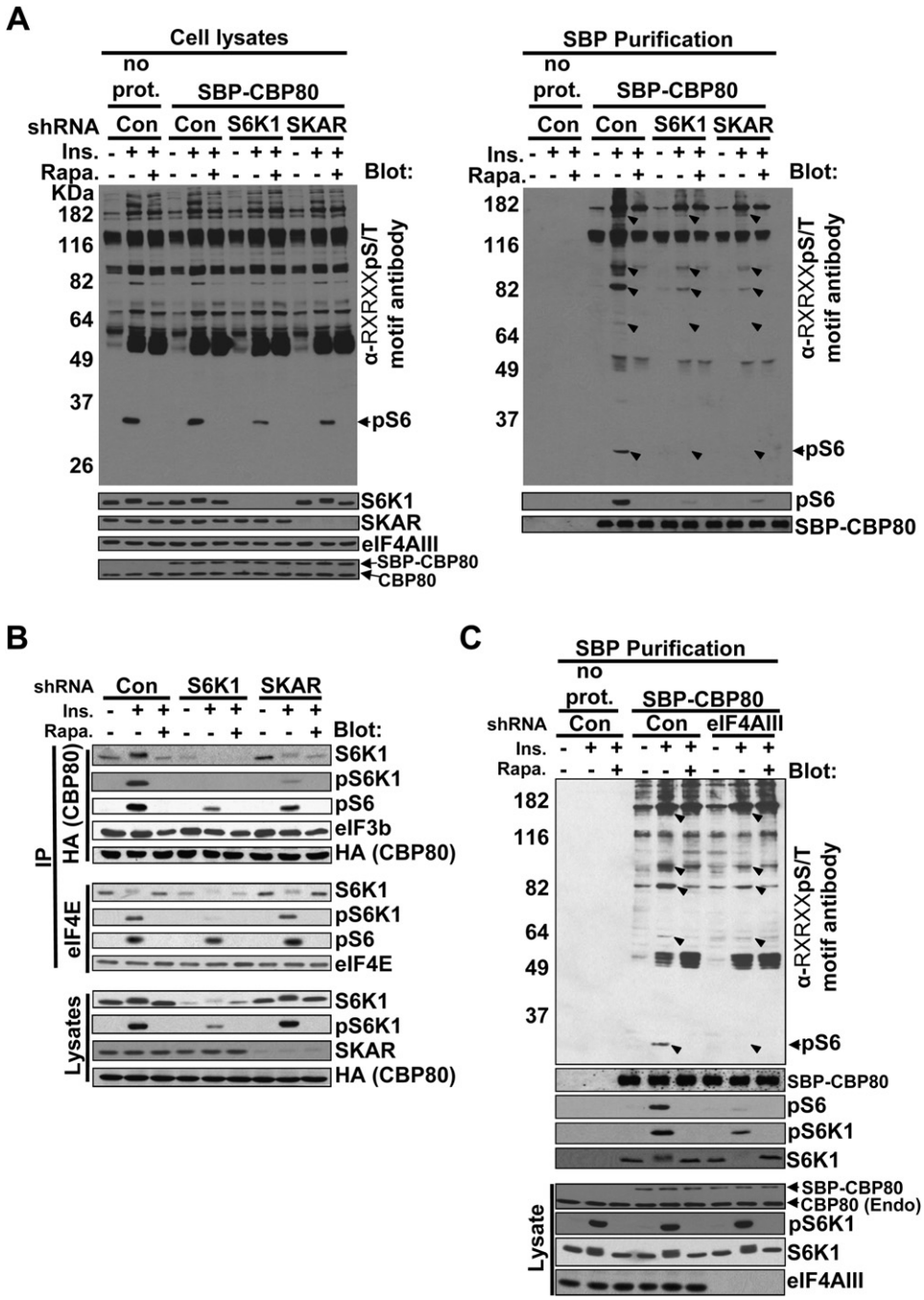

Figure 5. SKAR and eIF4AIII Mediate Phosphorylation of S6K1 Putative Targets in CBP80-Bound mRNPs

(A) Phosphorylation of putative S6K1 substrates in CBP80-bound mRNPs requires SKAR. HEK293E cells were infected with different shRNA-encoding viruses to induce RNAi-mediated gene-specific knockdowns. Forty-eight hours postinfection, cells were transfected with SBP-CBP80 plasmid or empty vector as control. Gene-specific knockdown was determined by immunoblotting with indicated antibodies, and the phosphorylation of putative S6K1 substrates in cell lysates was determined by anti-RXRXXpS/T motif antibody (left panels). CBP80-bound mRNPs were affinity purified using streptavidin-conjugated resin, and the phosphorylation of putative S6K1 substrates in the mRNPs was determined by anti-RXRXXpS/T motif antibody (right panel). Potential S6K1 substrates were indicated with arrowheads. Immunoblotting with anti-phospho-S6 (Ser 240/244) antibody was used to confirm the recognition of phospho-S6 by the motif antibody.

(B) The interaction between activated S6K1 and CBP80-bound mRNP is significantly reduced by RNAi depletion of SKAR. Gene specific knockdowns were prepared as described in (A). Cells were then transfected with HA-CBP80 plasmid. Forty-eight hours posttransfection, CBP80 and eIF4E-associated mRNPs were immunoprecipitated using anti-HA and anti-eIF4E antibodies, respectively. The presence of activated S6K1 in the mRNPs was determined by immunoblotting with the indicated antibodies.

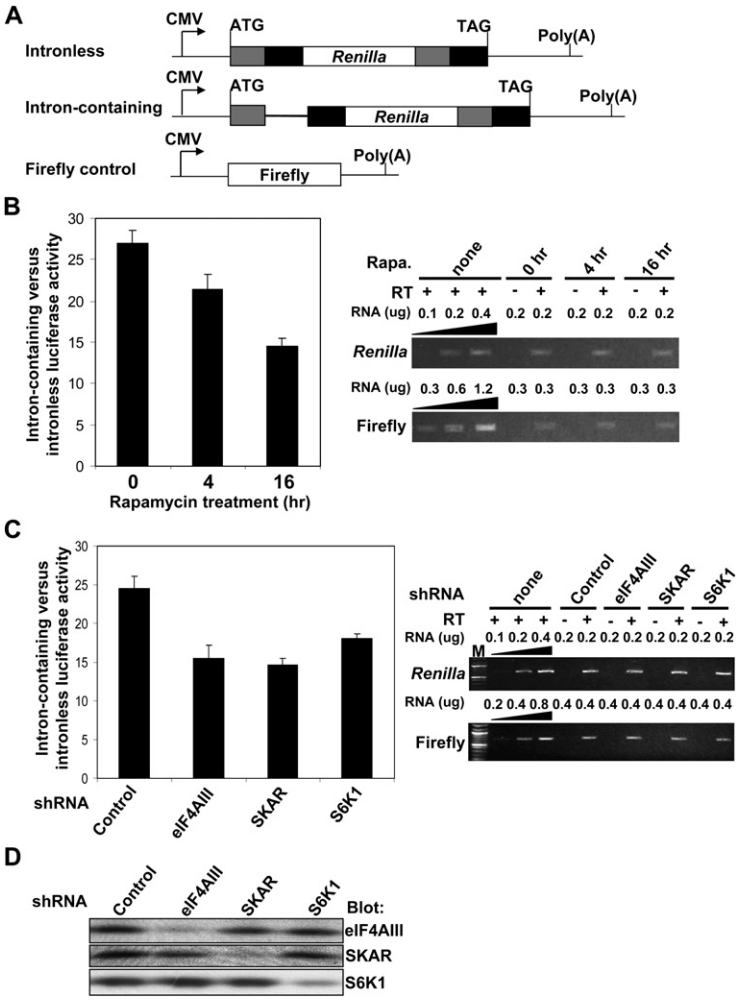

Figure 6. S6K1, SKAR, and eIF4AIII Contribute to the Enhanced Translational Yield Gained by Splicing

(A) Schematic of TPI/*Renilla* luciferase reporter constructs and Firefly control construct (Nott et al., 2003, 2004). TPI: the sixth intron and flanking exons from the human triose phosphate isomerase gene.

(B) Rapamycin antagonizes the enhanced translational yield gained by splicing. HEK293E cells were transfected with reporter constructs and serum starved. Forty-eight hours posttransfection, cells were stimulated with insulin or pretreated with rapamycin and stimulated with insulin for additional 4 or 16 hr. Luciferase activities were measured by a dual-luciferase assay. After normalization to the cotransfected firefly control, the intron-containing/intronless *Renilla* luciferase light unit ratio was calculated as described in Experimental Procedures. Experiments were carried out in triplicate. Data are presented as the mean ± SEM (left panel). mRNA levels of *Renilla* and Firefly genes were monitored using semiquantitative RT-PCR analysis (right panel). PCR reactions without reverse transcription (RT-) served as controls. A titration of RNA quantity used in PCR reactions served to ensure the PCR reactions were quantitative.

(C) S6K1, SKAR, and eIF4AIII modulate splicing-dependent enhancement of translation. HEK293E cells with gene-specific knockdowns were generated as in Figure 5. Cells were transfected with the reporter constructs and serum starved. 48 hr posttransfection, cells were stimulated with insulin. Luciferase activities were measured and calculated. Data are presented as the mean ± SEM (left panel). mRNA levels of *Renilla* and Firefly genes were monitored using semiquantitative RT-PCR (right panel).

(D) Reduction of individual gene expression induced by shRNA-mediated gene knockdown was determined by immunoblotting with the indicated antibodies.

SKAR as bait (unpublished data). Aly/REF also bridges the TREX complex to the 5′ CBC (Cheng et al., 2006). Although the details of these interactions have yet to be defined, these observations suggest that the 5′ CBC, the TREX complex, at least the first EJC, and proteins associated with the polyA tail may be in proximity to each other with the mRNA looping out between the various complexes. Thus activated S6K1 at the EJC may also be in proximity with targets in the CBC, the TREX complex and the polyA tail. Another possibility is that SKAR is also localized through Aly/REF to the TREX complex again positioning S6K1 near additional targets. Having S6K1 localized to these complexes provides the opportunity for S6K1 to phosphorylate multiple proteins which contribute to translation initiation. In addition, S6K1 localized at EJCs may also allow it to contribute to efficient translation elongation as the translational machinery proceeds along the mRNP and encounters each EJC. Future experiments are aimed at identifying the CBC-associated S6K1 targets and testing the above hypotheses.

While the CBC, the TREX complex and EJCs are removed from a newly synthesized mRNA during the pioneer round of translation (Ishigaki et al., 2001), how mTOR/S6K1 signaling are able to enhance overall translational yield is a question yet to be addressed. One possibility is that the first round of ribosome recruitment to the mRNA may have a significant impact on the efficiency of following rounds of ribosome recruitment. It is known that the initial ribosome recruitment is generally a rate-limiting step for translation in vivo (reviewed in Sonenberg, 1996). Therefore, an efficient pioneer initiation complex, mediated by the EJC and the mTOR signaling pathway, may promote steady state translation efficiency, which leads to increased protein synthesis. Another possibility is that the efficiency of mRNP remodeling, which occurs during or after the pioneer round of translation, may be modulated by mTOR/S6K1 signaling. A major mRNP remodeling event is the replacement of CBP80/20 by eIF4E at the 5′ cap (Ishigaki et al., 2001). While eIF4E is a limiting factor for steady state translation (reviewed in Sonenerg, 1996), its recruitment to the 5′ cap during mRNP remodeling events may be critical for efficient steady state translation. Thus, it will also be of interest to examine whether the mRNP remodeling as a result of the pioneer round of translation is regulated by the mTOR signaling pathway.

(C) Phosphorylation of putative S6K1 substrates in CBP80-bound mRNPs requires the EJC core protein eIF4AIII. RNAi-mediated knockdown of eIF4AIII, affinity purification of CBP80-bound mRNPs and immunoblotting were performed as described in (A) and (B). Potential S6K1 substrates were indicated with arrowheads.

EXPERIMENTAL PROCEDURES

Plasmids

pRK7-HA-SKAR and pRK7-HA-CBP80 were constructed by cloning full-length SKAR and CBP80, respectively, with an N-terminal hemagglutinin (HA) tag into pRK7 plasmid. pNTAP-CBP80 was constructed by cloning full-length CBP80 into pNTAP plasmid (Stratagene). The pSP72-AdML-M3, pSP72-AdMLΔi-M3 and pSP65-Ftz template constructs for in vitro transcription and the MS2-MBP fusion protein construct were provided by Robin Reed (Harvard Medical School, Boston, MA). Flag-tagged UPF3b and GFP-tagged hnRNP C1 were provided by Joan Steitz (Yale University School of Medicine, New Haven, CT). The TPI/Renilla and Firefly reporter constructs were provided by Melissa Moore (Brandeis University, Waltham, MA) and were described (Nott et al., 2003, 2004). Lentiviral plasmids (FSIPPW, Δ8.9, and VSVG) were provided by Andrew L. Kung (Dana-Farber Cancer Institute, MA) and David Baltimore (California Institute of Technology, CA).

Antibodies and Immunoblotting

Anti-SKAR antibodies were described previously (Richardson et al., 2004). Anti-SC35 and anti-Flag antibodies were purchased from Sigma. Anti-HA monoclonal antibodies were provided by Margaret Chou (University of Pennsylvania, Philadelphia, PA). Anti-Aly, anti-CBP80, and anti-eIF4AIII were generously provided by Robin Reed (Harvard Medical School, Boston, MA). Anti-eIF3b, anti-mTOR, and anti-Actin antibodies were purchased from Santa Cruz Biotechnology. Anti-S6K1, anti-S6, anti-phospho-S6 (Ser240/244), anti-eIF4E, and anti-RXRXXpS/T motif antibodies were purchased from Cell Signaling Technology. Proteins were resolved by SDS-PAGE, transferred onto nitrocellulose (Schleicher and Schuell), and probed with indicated antibodies. Data validating the specificity of antibodies used for immnoprecipitations in this study were included in Figure S1 by showing western blotting of a full-length gel.

Cell Lysis and mRNP Purification

Cell lysis and mRNP purification were performed according to Lejeune and Maquat (2004), with minor modifications. HEK293E cells from four 15cm dishes were lysed by sonication while suspended in 0.8mL of NET-2 (50 mM Tris-HCl, [pH 7.4]; 300 mM NaCl; 0.05% NP-40; 1 mM sodium vanadate, 40 μg/mL phenylmethyl sulfonyl fluoride [PMSF]; 0.5 μg/mL Leupeptin; 5 μg/mL Pepstatin) containing 100 U of RNase-inhibitor (Ambion). Details on antibody or affinity tag-based mRNP purification procedure were described in Supplemental Data.

Cell Culture, Transfection, and Splicing Extract Preparation

HEK293E cells were cultured and transfected as described (Holz et al., 2005). For experiments using starved, stimulated, and rapamycin treated conditions, cells were starved for 24 hr in DMEM, then either left untreated, stimulated with insulin (100 mM) for 30 min, or treated with rapamycin (20 ng/mL) for 20 min prior to insulin addition. Whole cell extracts containing splicing activities were prepared as described (Kataoka and Dreyfuss, 2004). For spliceosome assembly and purification analysis, pRK7-HA-SKAR plasmid was transfected into HEK293E cells twenty-four hours before splicing extracts were prepared. For the rest of the splicing-related reactions, the extracts were prepared from non-transfected HEK293E cells.

Spliceosome Assembly and Isolation

In vitro spliceosome assembly and affinity purification were performed according to (Zhou et al., 2002; Jurica et al., 2002) with modifications. Pre-mRNA or control mRNA (1.25 μg of each) containing MS2-binding sequences was incubated on ice with 100 μg of MS2-MBP protein for 20min, followed by spliceosome assembly under conditions optimized for splicing (total volume 0.75 mL). 100 μl amylose resin was used to affinity purify spliceosomes. Experimental details were described in Supplemental Data.

In Vitro Splicing and Immunoprecipitation

In vitro splicing reactions, analysis of splicing products, and immunoprecipitations were performed according to Le Hir et al. (2000), with minor modifications as described in Supplemental Data.

Construction of Site-Specific Radiolabeled RNA

AdML pre-mRNAs and control intronless mRNAs with site-specific radiolabel were constructed according to Ma et al. (2003). Briefly, AdML RNAs were site-specifically cleaved by RNase H in the presence of a specific 2′-O-methyl RNA-DNA chimeric oligonucleotide. 3′ half was subjected to a dephosphorylation reaction and followed by rephosphorylation at its 5′ end. The radiolabeled 3′ half RNA was then re-ligated with the 5′ half in the presence of a bridging DNA oligonucleotide and T4 DNA ligase. Experimental details were described in Supplemental Data.

Heterokaryon Assay and Immunofluorescence

The heterokaryon assay was performed according to (Pinol-Roma and Dreyfuss, 1992) with minor modifications as described in Supplemental Data.

Luciferase Assay

HEK293E cells were split into two wells, named w1 and w2, respectively in a 6-well plate. W1 was transfected with 0.5 μg of intron-containing TPI/*Renilla* luciferase plasmid plus 50 ng of Firefly control, while w2 was transfected with 0.5 μg intronless versions of TPI/*Renilla* luciferase plasmids plus 50 ng of Firefly control. Twenty-four hours posttransfection, cells were treated as described in different experiments, harvested, and the luciferase activity was measured by Turner Designs TD-20/20 dual-channel luminometer and Dual-Luciferase Reporter Assay System (Promega) according to the manufacturer's instructions. From w1 we obtained luciferase activities rw1 and fw1 representing *Renilla* luciferase and Firefly luciferase activities, respectively. Similarly, from w2 we obtain rw2 and fw2, respectively. Then the ratio of the intron-containing versus intronless TPI/*Renilla* gene expression was calculated by the equation ratio = (rw1/fw1) / (rw2/fw2).

RNA Interference

RNA interference was performed using lentiviral short hairpin RNA (shRNA) expression system as described in Supplemental Data.

RNA isolation and RT-PCR Analysis

RNA isolation and RT-PCR conditions and primer sequences were described in Supplemental Data.

SUPPLEMENTAL DATA

Supplemental Data include Supplemental Experimental Procedures, Supplemental References, and three figures and can be found with this article online at http://www.cell.com/cgi/content/full/133/2/303/DC1/.

ACKNOWLEDGMENTS

We thank Drs. Joan Steitz, Robin Reed, and Melissa Moore for their generous donation of plasmids and antibodies. We also thank members of the Blenis laboratory for discussions and critical reading of the manuscript (Michelle Mendoza, Max Hsia, Neil Kubica, and Andrew Choo). This work is supported by National Institutes of Health grant GM051405 (J.B.) and by the Leukemia and Lymphoma Society Fellowship 5597-07 (X.M.M.).

Received: May 16, 2007
Revised: October 26, 2007
Accepted: February 4, 2008
Published: April 17, 2008

REFERENCES

Braddock, M., Muckenthaler, M., White, M.R., Thorburn, A.M., Sommerville, J., Kingsman, A.J., and Kingsman, S.M. (1994). Intron-less RNA injected into the nucleus of Xenopus oocytes accesses a regulated translation control pathway. Nucleic Acids Res. *22*, 5255–5264.

Callis, J., Fromm, M., and Walbot, V. (1987). Introns increase gene expression in cultured maize cells. Genes Dev. *1*, 1183–1200.

Chang, Y.F., Imam, J.S., and Wilkinson, M.F. (2007). The nonsense-mediated decay RNA surveillance pathway. Annu. Rev. Biochem. *76*, 51–74.

Cheng, H., Dufu, K., Lee, C.S., Hsu, J.L., Dias, A., and Reed, R. (2006). Human mRNA export machinery recruited to the 5′ end of mRNA. Cell *127*, 1389–1400.

Chiu, S.Y., Lejeune, F., Ranganathan, A.C., and Maquat, L.E. (2004). The pioneer translation initiation complex is functionally distinct from but structurally overlaps with the steady-state translation initiation complex. Genes Dev. *18*, 745–754.

Dorrello, N.V., Peschiaroli, A., Guardavaccaro, D., Colburn, N.H., Sherman, N.E., and Pagano, M. (2006). S6K1- and betaTRCP-mediated degradation of PDCD4 promotes protein translation and cell growth. Science *314*, 467–471.

Dostie, J., and Dreyfuss, G. (2002). Translation is required to remove Y14 from mRNAs in the cytoplasm. Curr. Biol. *12*, 1060–1067.

Fingar, D.C., and Blenis, J. (2004). Target of rapamycin (TOR): an integrator of nutrient and growth factor signals and coordinator of cell growth and cell cycle progression. Oncogene *23*, 3151–3171.

Gingras, A.C., Raught, B., and Sonenberg, N. (1999). eIF4 initiation factors: effectors of mRNA recruitment to ribosomes and regulators of translation. Annu. Rev. Biochem. *68*, 913–963.

Gingras, A.C., Raught, B., and Sonenberg, N. (2001). Regulation of translation initiation by FRAP/mTOR. Genes Dev. *15*, 807–826.

Gudikote, J.P., Imam, J.S., Garcia, R.F., and Wilkinson, M.F. (2005). RNA splicing promotes translation and RNA surveillance. Nat. Struct. Mol. Biol. *12*, 801–809.

Hay, N., and Sonenberg, N. (2004). Upstream and downstream of mTOR. Genes Dev. *18*, 1926–1945.

Holz, M.K., Ballif, B.A., Gygi, S.P., and Blenis, J. (2005). mTOR and S6K1 mediate assembly of the translation preinitiation complex through dynamic protein interchange and ordered phosphorylation events. Cell *123*, 569–580.

Ishigaki, Y., Li, X., Serin, G., and Maquat, L.E. (2001). Evidence for a pioneer round of mRNA translation: mRNAs subject to nonsense-mediated decay in mammalian cells are bound by CBP80 and CBP20. Cell *106*, 607–617.

Izaurralde, E., Lewis, J., McGuigan, C., Jankowska, M., Darzynkiewicz, E., and Mattaj, I.W. (1994). A nuclear cap binding protein complex involved in pre-mRNA splicing. Cell *78*, 657–668.

Jurica, M.S., Licklider, L.J., Gygi, S.R., Grigorieff, N., and Moore, M.J. (2002). Purification and characterization of native spliceosomes suitable for three-dimensional structural analysis. RNA *8*, 426–439.

Kataoka, N., Diem, M.D., Kim, V.N., Yong, J., and Dreyfuss, G. (2001). Magoh, a human homolog of Drosophila mago nashi protein, is a component of the splicing-dependent exon-exon junction complex. EMBO J. *20*, 6424–6433.

Kataoka, N., and Dreyfuss, G. (2004). A simple whole cell lysate system for in vitro splicing reveals a stepwise assembly of the exon-exon junction complex. J. Biol. Chem. *279*, 7009–7013.

Kataoka, N., Yong, J., Kim, V.N., Velazquez, F., Perkinson, R.A., Wang, F., and Dreyfuss, G. (2000). Pre-mRNA splicing imprints mRNA in the nucleus with a novel RNA-binding protein that persists in the cytoplasm. Mol. Cell *6*, 673–682.

Le Hir, H., Izaurralde, E., Maquat, L.E., and Moore, M.J. (2000). The spliceosome deposits multiple proteins 20–24 nucleotides upstream of mRNA exon-exon junctions. EMBO J. *19*, 6860–6869.

Le Hir, H., Nott, A., and Moore, M.J. (2003). How introns influence and enhance eukaryotic gene expression. Trends Biochem. Sci. *28*, 215–220.

Lejeune, F., Ishigaki, Y., Li, X., and Maquat, L.E. (2002). The exon junction complex is detected on CBP80-bound but not eIF4E-bound mRNA in mammalian cells: dynamics of mRNP remodeling. EMBO J. *21*, 3536–3545.

Lejeune, F., and Maquat, L.E. (2004). Immunopurification and analysis of protein and RNA components of mRNP in mammalian cells. Methods Mol. Biol. *257*, 115–124.

Lejeune, F., and Maquat, L.E. (2005). Mechanistic links between nonsense-mediated mRNA decay and pre-mRNA splicing in mammalian cells. Curr. Opin. Cell Biol. *17*, 309–315.

Lejeune, F., Ranganathan, A.C., and Maquat, L.E. (2004). eIF4G is required for the pioneer round of translation in mammalian cells. Nat. Struct. Mol. Biol. *11*, 992–1000.

Lu, S., and Cullen, B.R. (2003). Analysis of the stimulatory effect of splicing on mRNA production and utilization in mammalian cells. RNA *9*, 618–630.

Ma, X., Zhao, X., and Yu, Y.T. (2003). Pseudouridylation (Psi) of U2 snRNA in S. cerevisiae is catalyzed by an RNA-independent mechanism. EMBO J. *22*, 1889–1897.

Matsumoto, K., Wassarman, K.M., and Wolffe, A.P. (1998). Nuclear history of a pre-mRNA determines the translational activity of cytoplasmic mRNA. EMBO J. *17*, 2107–2121.

Methot, N., Pickett, G., Keene, J.D., and Sonenberg, N. (1996). In vitro RNA selection identifies RNA ligands that specifically bind to eukaryotic translation initiation factor 4B: the role of the RNA remotif. RNA *2*, 38–50.

Nott, A., Le Hir, H., and Moore, M.J. (2004). Splicing enhances translation in mammalian cells: an additional function of the exon junction complex. Genes Dev. *18*, 210–222.

Nott, A., Meislin, S.H., and Moore, M.J. (2003). A quantitative analysis of intron effects on mammalian gene expression. RNA *9*, 607–617.

Palmiter, R.D., Sandgren, E.P., Avarbock, M.R., Allen, D.D., and Brinster, R.L. (1991). Heterologous introns can enhance expression of transgenes in mice. Proc. Natl. Acad. Sci. USA *88*, 478–482.

Pinol-Roma, S., and Dreyfuss, G. (1992). Shuttling of pre-mRNA binding proteins between nucleus and cytoplasm. Nature *355*, 730–732.

Reed, R., and Cheng, H. (2005). TREX, SR proteins and export of mRNA. Curr. Opin. Cell Biol. *17*, 269–273.

Richardson, C.J., Broenstrup, M., Fingar, D.C., Julich, K., Ballif, B.A., Gygi, S., and Blenis, J. (2004). SKAR is a specific target of S6 kinase 1 in cell growth control. Curr. Biol. *14*, 1540–1549.

Shibuya, T., Tange, T.O., Sonenberg, N., and Moore, M.J. (2004). eIF4AIII binds spliced mRNA in the exon junction complex and is essential for nonsense-mediated decay. Nat. Struct. Mol. Biol. *11*, 346–351.

Sonenberg, N. (1996). mRNA 5′ cap-binding protein eIF4E and control of cell growth. In Translation Control, J.W.B. Hershey, et al., ed. (Cold Spring Harbor, NY: Cold Spring Harbor Laboratory Press), pp. 245–269.

Tange, T.O., Nott, A., and Moore, M.J. (2004). The ever-increasing complexities of the exon junction complex. Curr. Opin. Cell Biol. *16*, 279–284.

Wang, W., Czaplinski, K., Rao, Y., and Peltz, S.W. (2001). The role of Upf proteins in modulating the translation read-through of nonsense-containing transcripts. EMBO J. *20*, 880–890.

Wiegand, H.L., Lu, S., and Cullen, B.R. (2003). Exon junction complexes mediate the enhancing effect of splicing on mRNA expression. Proc. Natl. Acad. Sci. USA *100*, 11327–11332.

Wilkinson, M.F. (2005). A new function for nonsense-mediated mRNA-decay factors. Trends Genet. *21*, 143–148.

Zhou, Z., Licklider, L.J., Gygi, S.P., and Reed, R. (2002). Comprehensive proteomic analysis of the human spliceosome. Nature *419*, 182–185.